GEOPHYSICAL RESEARCH LETTERS, VOL. 28, NO. 18, PAGES 3601-3604, SEPTEMBER 15, 2001

Discovery of a Water Vapor Layer in the Arctic Summer Mesosphere: Implications for Polar Mesospheric Clouds

Michael E. Summers

School of Computational Sciences, George Mason University, Fairfax, Virginia

R. R. Conway, C. R. Englert, D. E. Siskind, and M. H. Stevens

E. O. Hulburt Center for Space Research, Naval Research Laboratory, Washington, DC

J. M. Russell III

Center for Atmospheric Sciences, Dept. of Physics, Hampton University, Hampton, Virginia

L. L. Gordley and M. J. McHugh

GATS, Inc., Hampton, Virginia

Abstract. We report the discovery of a layer of enhanced water vapor in the Arctic summer mesosphere that was made utilizing two new techniques for remotely determining water vapor abundances. The first utilizes Middle Atmosphere High Resolution Spectrograph Investigation (MAHRSI) OH measurements as a proxy for water vapor. The second is a re-analysis of Halogen Occultation Experiment (HALOE) water vapor data with a technique to simultaneously determine polar mesospheric cloud (PMC) ice particle extinction along with the water vapor abundance. These results reveal a narrow layer of enhanced water vapor centered between 82-84 km altitude and coincident with PMCs, that exhibits water vapor mixing ratios of 10-15 ppmv. This indicates that a higher degree of supersaturation is present in the PMC region, and that PMCs are thus more efficient at sequestering total water (both ice particles and vapor) within the layer, than previously believed.

1. Introduction

Noctilucent clouds (NLCs) are Earth's highest clouds. They normally occur in the summer polar mesosphere for a period from about 6 weeks before to about 6 weeks after summer solstice and appear consistently in a thin 1-3 km layer between 80 and 85 km altitude (Thomas, 1991). They are typically observed poleward of about 50° latitude in both hemispheres although they have been sighted at lower latitudes to ~40°N. As observed from spacecraft these clouds are known as polar mesospheric clouds (PMCs). Because they form near the mesopause, where water vapor can become supersaturated, they have long been thought to be composed of water ice particles, as has been recently confirmed by HALOE IR spectral observations (Hervig et al., 2001). Although water vapor plays a central role in the formation and evolution of PMCs, measurements of water vapor with high vertical resolution within the PMC layer are lacking.

Copyright 2001 by the American Geophysical Union.

Paper number 2001GL013217.
0094-8276/01/2001GL013217$05.00

In this paper we discuss two new techniques for determining the water vapor distribution in the PMC region and show some key results, namely the discovery of a water vapor layer, coincident with PMCs, with mixing ratios significantly larger than found in the background mesosphere. The first of these methods involves using observed OH as a proxy for the water vapor abundance (H_2O is the source molecule for OH, see e.g. Brasseur and Solomon, 1986). Our earlier studies of MAHRSI OH data have been limited to low latitudes as sampled by the first MAHRSI mission in 1994 (Conway et al., 1996; Summers et al., 1997b). Those modeling studies confirmed the existence of a mesospheric water vapor layer at ~65-70 km altitude that had also been observed in HALOE water vapor data, and demonstrated that OH is a sensitive diagnostic of the water vapor distribution. It was also shown that the measured OH was inconsistent with standard odd-hydrogen photochemical theory (DeMore et al., 1997). In this paper we revisit both of these issues with high latitude MAHRSI OH data from its second mission in 1997. The second method is a new technique to simultaneously determine water vapor and PMC extinction from HALOE water vapor observations.

2. MAHRSI OH and Inferred Water Vapor

The OH, O_3 and temperature observations used in this study were obtained during the second flight of the CRISTA (Cryogenic Infrared Spectrometers and Telescopes for the Atmosphere) and MAHRSI experiments during August 8-16, 1997. MAHRSI measures solar resonance fluorescence of OH near 309 nm. Limb scans of this emission are inverted to obtain OH vertical density profiles (Conway et al., 1996; 1999). The CRISTA experiment employs three telescopes to measure infrared emission from several trace gases including O_3 and is also able to obtain atmospheric temperature (Stevens et al., 2001). Both instruments were mounted on the SPAS (Shuttle Pallet Satellite) that was deployed and retrieved by the space shuttle (STS-85). The inclination of the orbit was 57° and the co-aligned instruments were able to make observations up to about 71°N.

Inversion of individual MAHRSI limb scans of OH radiances yield vertical density profiles between 50 and 93

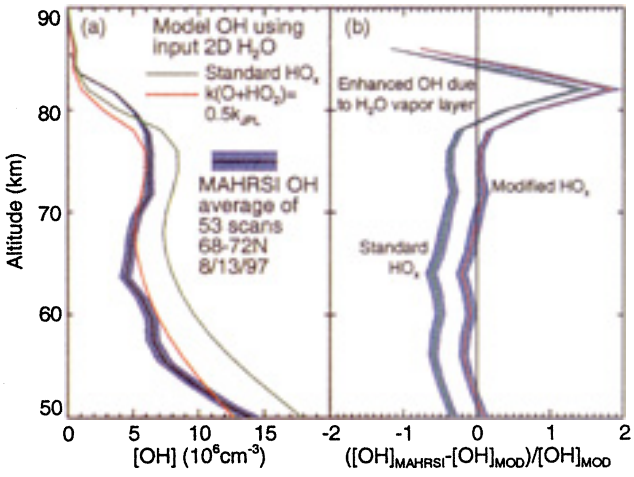

Figure 1. MAHRSI OH data from August 13-14,1997 between 68 - 71°N. Panel (a) shows the co-averaged 53 limb scans of OH along with 1-sigma measurement error, and model OH calculated assuming 2-D model H_2O profile shown in Figure 2. The OH inversion assumes an OH scale height of 2 km above 85.6 km. The scans included in the MAHRSI average are all between 9AM and 2PM local solar times. Model cases are shown for standard HO_x kinetics (DeMore et al., 1997) and with a 50% reduction for the rate coefficient of $O+HO_2 \rightarrow OH+O_2$. Panel (b) shows the difference between observed and model OH.

km altitude with a measurement uncertainty of less than 10% (Conway et al., 1996). During this mission the MAHRSI OH measurements at the highest northern latitudes revealed considerable OH variation along the orbital path. A portion of this variation is due to the dependence of OH upon solar zenith angle and local water vapor abundance (Summers et al., 1997b; Summers and Conway, 2000).

In this study we are primarily interested in the mean OH profile, and its implications for the vertical distribution of water vapor, at the highest latitudes sampled by MAHRSI. Scattering from PMC particles does not affect the MAHRSI OH measurements because the optical depth of PMCs at 309 nm is small and scattering from PMCs is broadband and only contributes to the background that is subtracted from the high spectral resolution OH emission lines. Here we focus only on those profiles between 68 - 71°N and 9am - 2pm local solar time, a time period over which the OH abundance shows relatively little diurnal variation. In Figure 1(a) we show the OH profile obtained from averaging 53 mid-day MAHRSI limb scans. The weighting function for this averaged profile has a width of 2 km at 82 km altitude. This profile exhibits the characteristic shape that was observed in MAHRSI OH from lower latitudes, i.e., a peak in the mid mesosphere, but here the peak is broader and shifted upward by about 8-10 km relative to that observed at lower latitudes (Summers and Conway, 2000).

In Figure 1(a) we show two model OH profiles obtained using the same photochemical model as used in our previous studies of the MAHRSI OH data (Summers et al., 1997b; Summers and Conway, 2000). In this model the water vapor is fixed to that obtained from a two dimensional chemical-dynamical model (Summers et al., 1997a) at the appropriate location and time of year of the MAHRSI observations. These model calculations also differ from that used earlier in that CRISTA O_3 between 60 and 95 km is used to constrain odd-oxygen chemistry, and CRISTA temperature measurements are used in the specification of the model atmosphere between 70 and 90 km (Stevens et al., 2001).

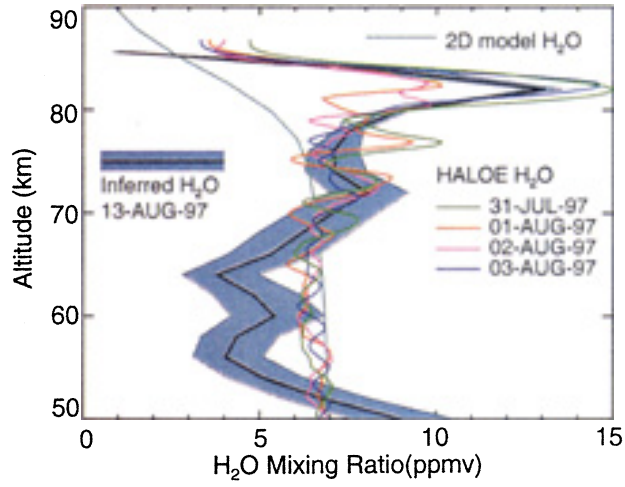

Figure 2. The H_2O profile inferred from MAHRSI OH is shown as the midline of the shaded area, which represents the inferred water vapor uncertainty obtained by inferring water vapor from the OH profile plus and minus the 1-sigma measurement error. The two-dimensional water vapor profile was obtained from the Summers et al. model (1997a). Also shown is re-processed (PMC corrected) H_2O from HALOE daily averaged occultations on July 31, August 1,2 and 3.

The standard photochemical model of OH shown in Figure 1(a) incorporates recommended kinetic rate coefficients (DeMore et al., 1997). We have shown in our earlier studies that standard HO_x chemistry substantially over predicts mesospheric OH densities in the lower mesosphere (Summers et al., 1997b) and we find the same result here. Also shown in Figure 1(a) is a model case where the reaction rate coefficient for $O + HO_2 \rightarrow OH + O_2$ is reduced by 50% from the standard recommendation. This rate change here leads to significantly better overall agreement between observed and modeled mid and lower mesospheric OH, thus we incorporate this rate change in subsequent models in this study. This change has also been shown to produce better agreement between model ozone and both HALOE and CRISTA ozone observations at the stratopause (Summers et al., 1997b).

As seen in Figure 1(a) the observed OH in the upper mesosphere is larger than that expected for an assumed water vapor profile that decreases monotonically above 70 km

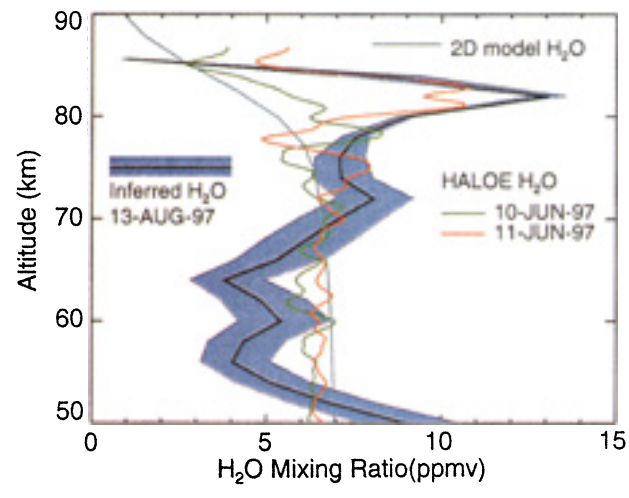

Figure 3. The same MAHRSI inferred and model H_2O as in Figure 2, but with HALOE (PMC-corrected) H_2O data from June 10 and 11, at 70°N and 66°N, respectively.

altitude (Summers and Conway, 2000). The difference between observed and modeled OH is shown in Figure 1(b). This altitude dependent difference is directly related to the difference between actual and assumed model water vapor. We demonstrate here that the actual atmospheric water vapor abundance can in fact be obtained from the measured OH density, using the photochemical model to relate the two.

The chemical loss of mesospheric water vapor is governed by a combination of ultraviolet photolysis from solar Lyman α radiation at 121.6 nm, mostly above 60 km altitude, and reaction between water vapor and $O(^1D)$ below that altitude. These processes, along with fast odd-hydrogen (HO_x = H + OH + HO_2) chemistry, produce OH and HO_2 radicals along with atomic hydrogen. In the mesosphere the chemical lifetime of water vapor ranges from about a day to several months, whereas the lifetime of OH is on the order of a minute. Thus OH is in photochemical equilibrium with water vapor.

Under conditions of photochemical equilibrium between odd-hydrogen and odd-oxygen (O_x = O + O_3) species, Allen et al. (1984) have shown that the production and loss equations can be solved algebraically for the O_3 abundance. Following their lead we can solve for the OH abundance in terms of the O_3 and H_2O, and we obtain an equation of the form

$$[OH] = a\,([O_3]\,[H_2O])^{1/2} \qquad (1)$$

where the brackets denote concentrations. The coefficient a is a function of the chemical rate coefficients that control OH/HO_2 partitioning and of the ozone photolysis rate that produces $O(^1D)$. Similarly, the O_3 abundance is a function of water vapor, i.e.,

$$[O_3] = b\,[H_2O]^{-1/3} \qquad (2)$$

Together, this implies that [OH] is proportional to $[H_2O]^{1/3}$. However, this assumes strict photochemical equilibrium and ignores contributions to HO_x/O_x chemistry from other chemical reactions. In the mesosphere, photochemical equilibrium is an accurate approximation below ~85 km altitude. Above that the downward transport of O from the lower thermosphere begins to contribute to the O_x budget. Also, additional chemical reactions contribute small amounts to HO_x chemistry primarily below ~55 km and above ~80 km altitude.

In order to determine H_2O from observed OH we assume a relationship between OH and H_2O of the form

$$[OH] = A\,[H_2O]^x \qquad (3)$$

However, in our methodology the values of A and x are determined by the photochemical model which includes all additional chemistry known to be important in the mesosphere that could potentially affect HO_x and O_x abundances, and also includes the downward transport of O from the upper atmosphere. In this study we have used the CRISTA O_3 measurements as a constraint on O_x between 70 – 90 km altitude, and tuned the downward transport of O, via a parameterized eddy diffusion coefficient, until the vertical profile of model O_3 matches the CRISTA O_3. The OH abundance depends approximately on the square root of the ozone abundance, thus an error in the O_3 abundance of 20% would then give an error in A of ~10%.

Using the above strategy we obtain the values of A and x, which are altitude dependent, from the photochemical model that incorporates an assumed water vapor distribution. The results we obtain show that x increases from ~0.4 near 50 km altitude (stratopause) to a peak of ~1.4 at 82 km and falls to ~0.8 at 86 km altitude. In Figure 2 we show the inferred water vapor, i.e., its abundance obtained from equation (3) using the model determined A's and x's, along with the observed OH. In order to insure self-consistency, as an intermediate step we used the inferred water vapor to calculate new A's and x's and these were virtually identical to the initial values. The sharp peak in water vapor near 82 km is a robust feature of this procedure.

3. HALOE H_2O Observations

The HALOE experiment aboard the NASA Upper Atmospheric Research Satellite (UARS) uses both broadband and gas correlation radiometry (Russell et al., 1993). Included in its suite of measurements are broadband transmission channels targeted for H_2O and NO_2. Current HALOE water vapor data (V.19) near the high latitude summer mesopause contain extinction from both water vapor and ice particles whenever PMCs appear in the line-of-sight. To accurately determine water vapor in the vicinity of PMCs, we developed an improved retrieval technique that accounts for PMC extinction. In this process we iteratively retrieve three quantities: PMC extinction from the 6.26 μm channel, temperature from the 2.80 μm channel and water vapor from the 6.62 μm channel. Water vapor, carbon dioxide and PMC particles, respectively, dominate the extinctions in these three wavebands above 70 km. We determine the PMC extinction in other channels using the extinction retrieved at 6.26 μm and assuming a wavelength dependence calculated from Mie scattering due to small ice particles. Hervig et al. (2001) have confirmed this ice spectrum experimentally.

In HALOE V.19 production retrievals, the transmission signals are first smoothed in altitude to improve signal-to-noise. But because PMC layers are expected to be thin (1-3 km), this smoothing is omitted in the PMC correction process that we utilize here. Because the transmission signals at these altitudes are very small, and because the 6.26 μm channel has relatively low signal to noise, another means of noise reduction is needed. This is achieved by using daily average transmission signals. (There are nominally 15 occultations per day, in a narrow latitude band). The systematic error for single profile water vapor retrievals is ~10% above the stratopause, and the random error for daily averaged retrievals is ~0.7 ppmv.

In Figure 2 we show PMC-corrected HALOE water vapor for four daily averages closest in time and latitude to the MAHRSI OH measurements. The HALOE results dramatically confirm the peak in water vapor near 82 km. On two days HALOE observed peak values almost identical to the MAHRSI inferred mixing ratio of ~15 ppmv, and on the other two days they are lower by ~5 ppmv. Figure 3 shows reprocessed HALOE water vapor from June 10 and 11, early in the PMC "season" and whereas the June 11 data show a peak near 82 km, data from June 10 shows a water vapor distribution that is more similar to the two-dimensional model result shown in Figure 2. There is a systematic 1-2 sigma difference between inferred H_2O and HALOE H_2O in the 53-67 km altitude region that is not yet understood.

4. Discussion

Our results show that the Arctic summer mesospheric region between 82 and 85 km concentrates water. The ultimate source of this water is upwelling from below. This suggests significant dehydration of the air above 85 km relative to that below 82 km. Above the ~83 km peak the

water vapor abundance decreases from near 15 ppmv to less than 5 ppmv at 85 km and indicates that the water vapor scale height in this region is ~ 3 km. This suggests that a large fraction of the water vapor flowing vertically through the 82-85 km region is sequestered within the layer as either vapor or ice. Given a typical vertical advection velocity (Garcia, 1989; Summers et al., 1997a) of ~1cm/s, it takes the upwelling air ~3 days to flow through the region. Absent other loss processes (e.g. photolysis) this implies a sequestering rate of 2-3 ppmv (water vapor + equivalent evaporated ice) per day. Thus in only a few days an enhanced water vapor layer can be produced, although upwelling continues throughout the PMC season. The peak water vapor mixing ratio will continue to increase until a balance is reached between this feeding of water vapor from upwelling air and loss by photolysis and diffusion.

Our results of enhanced water vapor at the 10-15 ppmv level, coincident with the PMC region, are consistent with the indirect estimates of von Cossart et al (1999) who speculated that the total amount of water (ice) contained in NLCs would produce ~12 ppmv water vapor if distributed over a narrow layer, as we report here. This peak in water vapor is significantly larger than typical mesospheric water vapor abundances and indicates a higher degree of supersaturation in the PMC region than previously inferred using modeled water vapor (Thomas, 1991; Lübken, 1999) or obtained from ground-based water vapor observations with lower vertical resolution (Seele and Hartogh, 1999).

The enhanced layer also implies strong coupling between water vapor and ice particles (Thomas, 1991). Although the overall importance of sedimentation is controversial (Klostermeyer, 1998; Chu et al., 2001), the evaporation of ice particles at the base or just below the PMC layer will elevate the water vapor abundance of air upwelling into the ice particle nucleation/formation region and this positive feedback magnifies the water vapor supersaturation in the ice particle growth region. This has important implications for the time scales of PMC/NLC growth and decay. Jensen and Thomas (1994), using a water vapor mixing ratio at 82 km of 1 ppmv, obtained a growth time scale of 1-2 days. Klostermeyer (1998), using 4.5 ppmv, obtained a time scale of only a few hours and suggested that condensation and sublimation occur more rapidly than sedimentation. Our observations of 10-15 ppmv suggest that even the Klostermeyer timescale may be too long. Further progress in understanding the relative roles of PMC nucleation, condensation, sedimentation and sublimation would greatly benefit from long term, global observations of water vapor at both the mesopause and PMC/NLC altitudes.

Acknowledgments. We thank J. G. Cardon for his help with analysis of the MAHRSI OH observations and M. Kaufmann for providing CRISTA O_3 data. We also express our gratitude to G. E. Thomas and J. Gumbel for useful discussions on PMCs. This work was supported by the NASA offices of Space Science and Earth Science and in part by the Office of Naval Research. This work was performed while C. R. Englert held a National Research Council – NRL Research Associateship.

References

Allen, M., J.I. Lunine, and Y.L. Yung, The Vertical Distribution of Ozone in the Mesosphere and Lower Thermosphere, *J. Geophys. Res.*, 89, 4841-4872, 1984.

Brasseur, G. and S. Solomon, Aeronomy of the Middle Atmosphere, Reidel, Dordrecht, Netherlands, 1986.

Chu, X., C.S. Gardner, and G. Papen, Lidar Observations of Polar Mesospheric Clouds at the South Pole: Diurnal Variations, *Geophys. Res. Lett.*, 28, 1937-1940, 2001.

Conway, R.R. et al., Satellite measurements of hydroxyl in the mesosphere, *Geophys. Res. Lett.*, 23, 2093-2096, 1996.

Conway, R.R. et al., The Middle Atmosphere High Resolution Spectrograph Investigations, *J. Geophys. Res.*,104, 16,327-16,348, 1999.

DeMore, W.B., et al., Chemical Kinetics and Photochemical Data for use in Stratospheric Modelling, Evaluation No. 12, Publ. 97-4, Jet Propulsion Laboratory, Pasadena, CA 1997.

Garcia, R.R., Dynamics, Radiation, and Photochemistry in the Mesosphere: Implications for the Formation of Noctilucent Clouds, *J. Geophys. Res.*, 94, 14,605-14,515, 1989.

Hervig, M.E., et al., First confirmation that water ice is the primary component of polar mesospheric clouds, *Geophys. Res. Lett,* 28, 971-974, 2001.

Jensen, E. and G.E. Thomas, Numerical simulations of the effects of gravity waves on noctilucent clouds, *J. Geophys. Res.*, 99, 3421-3430,1994.

Klostermeyer, J., A simple model of the ice particle size distribution in noctilucent clouds, *J. Geophys. Res.*,103, 28743-28752, 1998.

Lübken, F.-J., Thermal structure of the Arctic summer mesosphere, *J. Geophys. Res.*, 104, 9135-9149, 1999.

Stevens, M.H., et al., On the Water Frost Point in the Arctic Summer Mesosphere, submitted to Geophys. Res. Lett. (2001).

Russell, J.M., III et al., The Halogen Occultation Experiment, *J. Geophys. Res.*, 98, 10,777-10,797, 1993.

Seele, C. and P. Hartogh, Water vapor of the polar middle atmosphere: Annul variation and summer mesospher conditions as observed by ground-based microwave spectroscopy, *Geophys. Res. Lett.*, 26, 1517-1520, 1999.

Summers, M.E. et al., The Seasonal Variation of Middle Atmospheric CH4 and H2O with a new chemical-dynamical model, *J. Geophys. Res.*, 102, D3, 3503-3526, 1997a.

Summers, M.E., et al., Implications of Satellite OH Observations for Middle Atmopsheric H_2O and Ozone, *Science*, 277, 1967-1970, 1997b.

Summers, M.E. and R.R. Conway, Insights into Middle Atmospheric Hydrogen Chemistry from Analysis of MAHRSI OH Observations, AGU Monograph #123, *Atmospheric Science Across the Stratopause*, 117-130, 2000.

Thomas, G.E., Mesospheric Clouds and the Physics of the Mesopause Region, *Rev. of Geophys.*, 29, 553-575, 1991.

von Cossart, G., J. Fiedler, and U. von Zahn, Size distributions of NLC particles as determined from 3-color observations of NLC by ground-based lidar, *Geophys. Res. Lett.*, 26, 1513, 1999.

M. E. Summers, School of Computational Sciences, Department of Physics and Astronomy, and Center for Earth Observing and Space Research, George Mason University, MSN-5C3, Fairfax, VA 22030; email: msummers@physics.gmu.edu.

R. R. Conway, C. R. Englert, M. H. Stevens, D.E. Siskind, E. O. Hulburt Center for Space Research, Naval Research Laboratory, Washington, DC 20375

J. M. Russell III, Department of Physics, Hampton University, Hampton, VA 23668

L. L. Gordley, M. McHugh, GATS, Inc., Hampton, VA 23666.

(Received March 23, 2001; revised June 21, 2001; accepted June 21, 2001.